Effects of including radial velocity on a storm simulation

Lee, SeonYong[1], Hye-Yeong Chun[2], Chun-Ho Cho[1]

(1) National Institute of Meteorological Research/KMA, Seoul 156-720, Korea

(2) Department of Atmospheric Sciences, Yonsei University, Seoul,120-749, Korea.

1. Introduction

High-resolution Doppler radar data made it possible to analyze the structure of storms in detail. From this possibility, there have been many researches to apply the radar date to initial condition of the numerical weather prediction. Xiao and Sun (2007) examined the impact of multiple-Doppler radar data assimilation on quantitative precipitation forecasting (QPF) using a three-dimensional variational data method (3DVAR) of the Weather Research and Forecast model (WRF 3DVAR) for a squall-line convection simulation. Hu and Xue (2007) examined the impact of the radial velocity of the WSR-88D radar data on a tornadic thunderstorm by applying various assimilation procedures with the 3DVAR in Advanced Regional Prediction System (ARPS 3DVAR). Besides recent variational or EnKF methods of applying the radar data to data assimilation process, there are more simple and fast classic assimilation methods, such as, Barnes's (1964) and Bratseth's (1986) methods, which are adapted in ARPS Data Assimilation System (ADAS) (Brewster, 1996) and Local Analysis and Prediction System (LAPS) (Albers, 1995).

Recently Korea Meteorological Administration (KMA) upgraded its operation radar system by using nine upgraded S-band radars including two WSR-88D radars of the US Air Forces in Korea. In the upgraded radar system, KMA can get reasonable radial velocity data in 10 minutes interval.

In the present research, we coupled the objective analysis system, LAPS, to the forecast system, WRF, through the WRF Standard Initialization (WRFSI) process, and the radial velocity data of the S-band radar are ingested into the LAPS wind analysis process. Effects of the radial velocity on the simulation of a storm on the monsoon front are investigated by comparison of the results with and without the radial velocity in LAPS.

2. Data and Method

To examine the effect of radial velocity, we choose a storm on the Ease Asian Monsoon front, called Jangma front in Korea, which occurred on July 1, 2005. Figure 1 is the surface chart (left) at 15 UTC July 1, 2005 and the infrared image of the GOES-9 satellite at 16 UTC (right). In the surface chart, the stationary Jangma front exists from east coast of China through southern part of the Korean Peninsula to the main land of Japan, and the clusters of storms exist along this front as in the satellite image. The northwesterly wind driven by the low pressure system at the north of the Korean Peninsula and the southwesterly wind driven by the west boundary of the Northwest Pacific High converge in the Korean part of the Jangma front, and this produces storm clusters as seen in the satellite image. The storm of our interest is the one in the circle at the satellite image, which is organized during the period between 15 UTC and 16 UTC on this day.

Corresponding address: SeonYong Lee, National Institute of Meteorological Research/KMA, Seoul 156-720, South Korea, sylee@metri.re.kr.

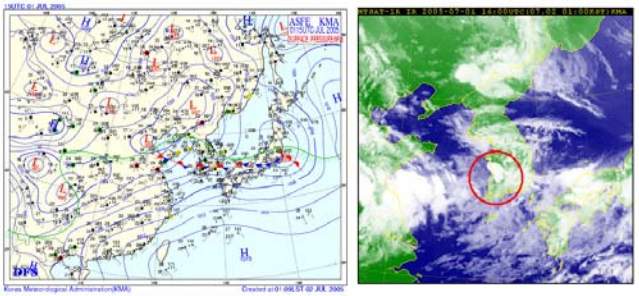

Fig. 1 *The synoptic environment at 15 UTC July 1, 2005. The left one is the surface chart issued by KMA and the right one is the infrared image of the GOES-9 satellite at 16 UTC on this day. The circle at the satellite image is the target storm cluster of our research.*

The evolution of the target storm is seen in Fig. 2. The storm was initiated at the west coast of the Korean peninsula at 14 UTC, organized into a line of convective cell until 15 UTC, developed into a squall line type storm at 16 UTC, and a supercell was developed in the leading part of the squall line at Jangsu, the upstream part of Mt. Duck-yu, at 17 UTC.

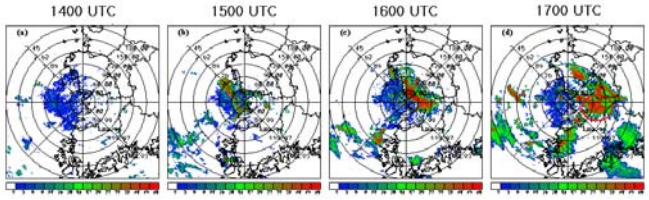

Fig. 2 *The plan position indicators (PPI) of reflectivity factor at 0.5 degree elevation of the Gunsan WSR-88D radar from 1400 UTC to 1700 UTC July 1, 2005 in 1 hour interval.*

We ingested the radial velocity and reflectivity data of Gunsan WSR-88D radar at 1700 UTC into the LAPS. In the LAPS, the radial velocity is first mapped into the LAPS grid and then the tangential wind component is calculated from the background wind at the grid where the radial velocity is obtained. The next step is to combine the mapped radial velocity and the calculated tangential wind components to produce a wind vector (Albers, 1995). The reflectivity factor is also mapped into grid points and utilized at the cloud and moisture analysis.

Figure 3 is the radial velocities of Gunsan and Pyeongtaek WSR-88D radars and the Jindo KMA radar with the analyzed wind vector and the initial condition of

the WRF forecast. The strong shears in the circles of the panels (a), (b) and (d) indicate the existence of the meso-cyclone at Jangsu area. The analyzed horizontal wind fields of the (e) and (f) panels show that a strong wind convergence exists upstream of the supercell area.

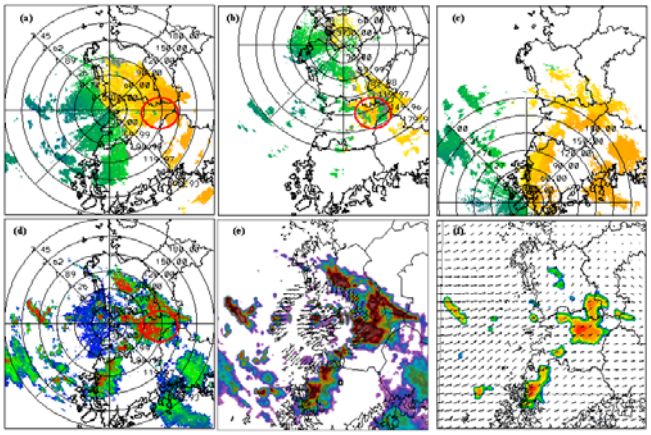

Fig. 3 *(a) The radial velocity from Gunsan WSR-88D radar at 1700 UTC July 1, 2005. The circled area indicates the existence of a meso-cyclone. (b) The radial velocity at Pyeongtaek WSR-88D. (c) The radial velocity at Jindo S-band radar. (d) The reflectivity factor at Gunsan radar. (e) The analyzed wind vector and reflectivity with respect to the Gunsan radar. (f) The simulated reflectivity and the horizontal wind fields on the 925 hPa surface at the 2 minutes forecast of the WRF from the initial time, 1700 UTC.*

The storm was simulated using a meso-scale model WRF with the input data from LAPS. The domain of the integration is shown in Fig. 4 where the round dot is the Gunsan radar site and the square dot is the Jangsu area. The horizontal resolution is 3 km and the numbers of grids are 151x151x39 in x, y, and z directions, respectively. The top pressure of the model domain is 50 hPa. Two simulations are conducted with and without the radial velocity in LAPS.

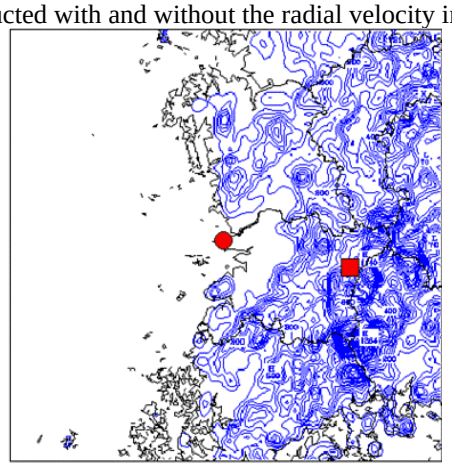

Fig. 4 *Domain of the WRF simulation. The round dot is the Gunsan radar site and the square dot is the Jangsu area.*

3. Results

Compared with the simulation result without the radial velocity, effects of including the radial velocity on the simulated storms appeared in two ways. First, the wind speed at low level increases while that at upper level decreases as in Fig. 5. This is because the radar retrieved wind assimilated in the initial condition is stronger and more convergent at low level but weaker at upper level. The convective cells exist from the initial time step of the integration for the with-radar-data case, but the moisture field appeared at upper level only for the without-radar-data case.

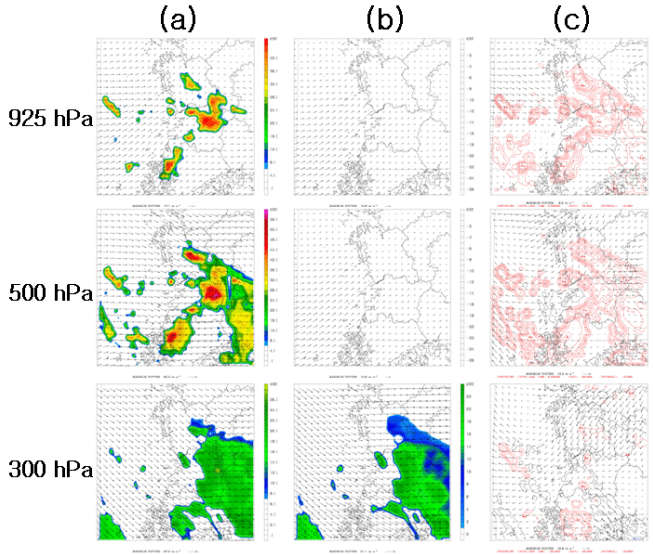

Fig. 5 *The one minutes forecast from 17 UTC on July 1, 2005. The panels in the column (a) are with-radar-case, those of the column (b) are without-radar-data case, and the panels in the column (c) are the difference the with-radar-data case from without-radar-data case. The shades are the synthesized radar reflectivity from hydrometers. The contours in (c) are the difference of the reflectivity factor in 5 dBZ interval and the red one is positive and the blue one is negative.*

Second, more convective cells are produced in the with-radar-data case as in the Fig. 6. At Fig. 6, we can see that many small convective cells are developed for the with-radar-data case, while a few intense convective cells are produced at for the without-radar-data case. This is because storm relative helicity at the initial condition is larger for the with-radar-data case as in the Fig. 7. The relative helicity of the storm becomes higher due to the enhanced low level wind shear in the initial condition. Consequently, under this higher storm relative helicity, the convective cells are more easily trigged than the without-radar-data case.

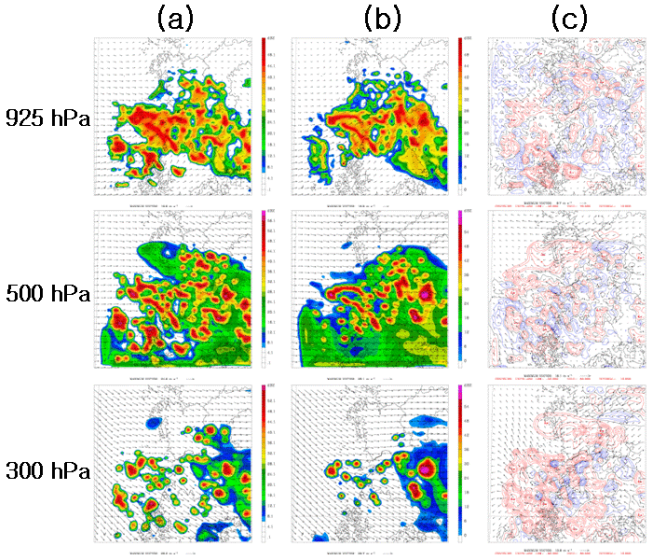

Fig. **6** *The 40 minutes forecast from 17 UTC on July 1, 2005. Others are the same as Fig. 5.*

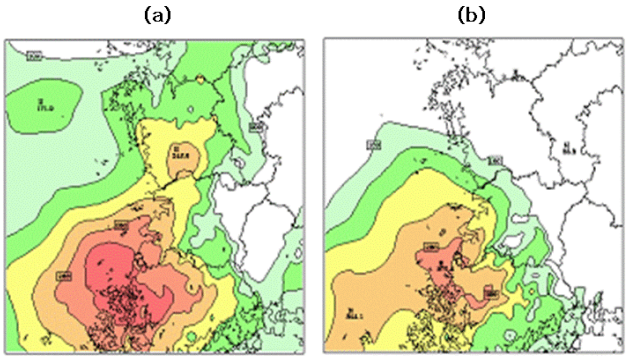

Fig. 7 *Storm relative helicity at the one minutes forecast from 17 UTC July 1, 2005. The panel (a) is the with-radar-data case and the panel (b) is the without-radar-data case. The interval of contours is 40* m^2s^{-2}.

Comparison of the hourly precipitation of WRF with the observation from the Automatic Weather Stations (AWS) of KMA shows that the result of the simulation including the radial velocity is better than that without the radial velocity as in the Fig. 8.

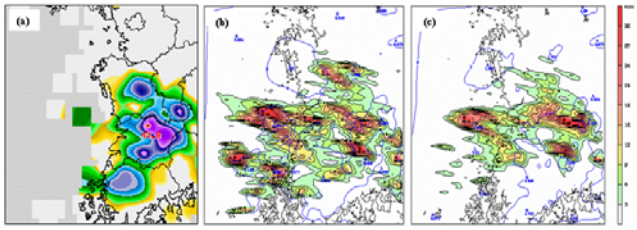

Fig. 8 *Comparison of the one hour forecast with the AWS data. (a) is the AWS rain rate data, (b) is the rain rate of the with-radar-data case, and (c) is that of the without-radar-data case.*

4. Summary

1) The impact of the radar data on a storm on the monsoon front was investigated, by comparison of the simulations with and without the radial-velocity data in the initialization process.
2) The wind speed at low level increases while that at upper level decreases by including the radial velocity.
3) More convective cells are produced for the with-radar-data case, while a few intense convective cells were developed for the without-radar-data case.
4) The storm relative helicity is larger for the with-radar-data case than the with-radar-data case
5) Comparison of the hourly precipitation of WRF with the AWS data of KMA shows that the result of the simulation including the radial velocity is better than that without the radial velocity.

Acknowledgment

This research is supported by the “Study on the Weather Radar Application” project of the National Institute of Meteorological Research of Korea Metrological Administration.

References

Albers, S. C., 1995; The LAPS wind analysis. *Wea. Forecasting*, **10**, 342-352.

Barnes, S. L., 1964; A technique for maximizing details in numerical weather map analysis. *J. Appl. Meteor*., **3**, 396-409.

Bratseth, A. M., 1986; Statistical interpolation by means of successive corrections. *Tellus*, **38A**, 439-447.

Hu, M. and M. Xue, 2007; Impact of configurations of rapid intermittent assimilation of WSR-88D radar data for the May 2003 Oklahoma city tornadic thunderstorm case. *Mon. Wea. Rev.*, **135**, 507-525.

Xiao, Q. and J. Sun, 2007; Multiple-radar data assimilation and short-range quantitative precipitation forecasting of a squall-line observation during IFOP_2002. *Mon. Wea. Rev*., **135**, 3381-3404.